J|A|C|S
ARTICLES
Published on Web 11/24/2005

Theoretical Study of the ^{13}C NMR Spectroscopy of Single-Walled Carbon Nanotubes

Nicholas A. Besley,* Jeremy J. Titman, and Matthew D. Wright

Contribution from the School of Chemistry, University of Nottingham, University Park, Nottingham, NG7 2RD, U.K.

Received September 5, 2005; E-mail: nick.besley@nottingham.ac.uk.

Abstract: The ^{13}C NMR spectroscopy of armchair and zigzag single-walled carbon nanotubes has been investigated theoretically. Spectra for (4,4), (5,5), (6,6), (6,0), (9,0), and (10,0) nanotubes have been simulated based on ab initio calculations of model systems. The calculations predict a dominant band arising from the carbon atoms in the "tube" with smaller peaks at higher chemical shifts arising from the carbon atoms of the caps. The dominant band lies in the range of 128 and 138 ppm. Its position depends weakly on the length, width, and chirality of the tubes. The calculations demonstrate how structural information may be gleaned from relatively low-resolution nanotube ^{13}C NMR spectra.

Introduction

Since the discovery of multiwall[1] and single-wall carbon nanotubes[2] (SWNTs), there has been an intensive effort toward characterizing and understanding their properties. Much of this interest arises from the diverse nature of their chemical and physical properties, which depend on structural parameters such as width and helicity.[3,4] This has led to much speculation about potential applications. These range from electronic devices to biotechnology. However, to realize this potential requires the synthesis and preparation of nanotubes with a well-defined structure.

A SWNT can be viewed as a rolled graphene sheet and is classified by a vector connecting the two points that meet upon rolling. There are three classes of nanotube: armchair, zigzag, and chiral. These are labeled by (n,n), $(n,0)$, and (n_1,n_2), respectively. A variety of techniques are used to characterize nanotube samples. These include scanning tunneling microscopy,[3] optical absorption,[5] fluorescence spectroscopy,[6] and Raman scattering.[7] However, these methods even in combination do not provide a full characterization. Consequently, alternative techniques that provide a more detailed description need to be found. One possibility is ^{13}C nuclear magnetic resonance (NMR) spectroscopy.

Measurement of the ^{13}C NMR spectrum of nanotubes is problematic due to residual ferromagnetic and paramagnetic impurities from the catalyst used in the synthesis of the tubes. These impurities lead to a very large broadening of the NMR signal. Despite these difficulties, several groups have reported measurements of nanotube ^{13}C NMR.[8−11]

Tang et al. reported static and magic angle spinning (MAS) ^{13}C NMR spectra of SWNTs.[8] A broad signal was obtained with an isotropic shift of 124 ppm with respect to tetramethylsilane (TMS). Two types of nanotube were identified through differences in ^{13}C spin−lattice relaxation time. A fast-relaxing component was assigned to metallic tubes, while semiconducting tubes have a slow relaxation time. For metallic tubes, the Knight shift was small in comparison to the chemical shift. In a subsequent study,[12] baking at high temperature was used to remove the ferromagnetic impurities. A band at 126 ppm with width at half-maximum of 50 ppm was obtained. The broadening was attributed to the distribution of isotropic shifts of inequivalent carbons. Such a baking process can modify the sample. Consequently, nanotubes were prepared with a nonferromagnetic catalyst. A MAS spectrum with peak at 126 ppm was obtained. Only a weak dependence of line shape on both tube radius and chirality was found, and it was postulated that NMR could resolve electronic properties but not structural properties.[9]

Hayashi et al.[10] reported ^{13}C NMR MAS spectra of SWNTs with a chemical shift of 116 ppm and width of 30 ppm. In addition, small peaks at 171 and 152 ppm were observed. These peaks were tentatively assigned to carbon species at edges or defects, in particular, to COOH and C−OH groups by analogy with the ^{13}C NMR of benzoic acid and phenol. The broadening

(1) Iijima, S. *Nature* **1991**, *354*, 56−58.
(2) Iijima, S.; Ichihashi, T. *Nature* **1993**, *363*, 603−605.
(3) Wilder, J. W. G.; Venema, L. C.; Rinzler, A. G.; Smalley, R. E.; Dekker, C. *Nature* **1998**, *391*, 59−62.
(4) Odom, T. W.; Huang, J. L.; Kim, P.; Lieber, C. M. *Nature* **1998**, *391*, 62−64.
(5) Marinopoulos, A. G.; Reining, L.; Rubio, A.; Vast, N. *Appl. Phys. A* **2004**, *78*, 1157−1168.
(6) Weisman, R. B.; Bachilo, S. M.; Tsyboulski, D. *Appl. Phys. A* **2004**, *78*, 1111−1116.
(7) Dresselhaus, M. S.; Dresselhaus, G.; Saito, R.; Jorio, A. *Phys. Rep.* **2005**, *409*, 47−99.
(8) Tang, X.-P.; Kleinhammes, A.; Shimoda, H.; Fleming, L.; Bennoune, K. Y.; Sinha, S.; Bower, C.; Zhou, O.; Wu, Y. *Science* **2000**, *288*, 492−494.
(9) Goze-Bac, C.; Latil, S.; Lauginie, P.; Jourdain, V.; Conard, J.; Duclaux, L.; Rubio, A.; Bernier, P. *Carbon* **2002**, *40*, 1825−1842.
(10) Hayashi, S.; Hoshi, F.; Ishikura, T.; Yumura, M.; Ohshima, S. *Carbon* **2003**, *41*, 3047−3056.
(11) Kitaygorodskiy, A.; Wang, W.; Xie, S.-Y.; Lin, Y.; Shiral Fernando, K. A.; Wang, X.; Qu, L.; Chen, B.; Sun, Y.-P. *J. Am. Chem. Soc.* **2005**, *127*, 7517−7520.
(12) Goze Bac, C.; Latil, S.; Vaccarini, P.; Bernier, P.; Gaveau, P.; Tahir, S.; Micholet, V.; Aznar, R.; Rubio, A.; Metenier, K.; Beguin, F. *Phys. Rev. B* **2001**, *63*, 100302.

10.1021/ja055888b CCC: $30.25

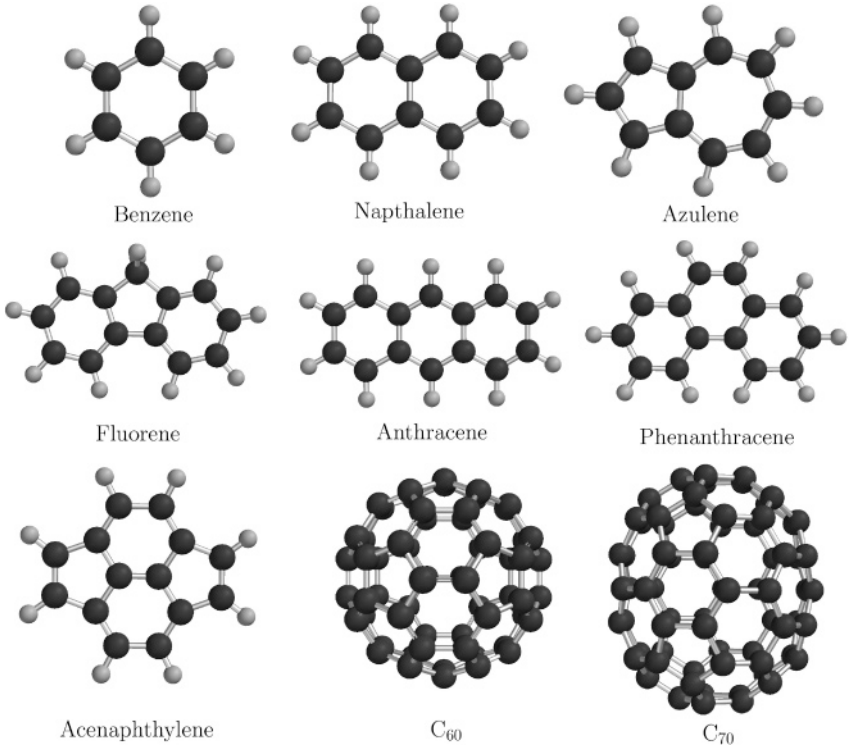

Figure 1. Test set of molecules.

of the spectral line was attributed to the distribution of diameters and helicities. Furthermore, ^{1}H NMR spectra revealed a high concentration of H-containing species; about 10% of carbons were associated with H-containing species.

In a recent study, the ^{13}C NMR of functionalized nanotubes in solution phase was reported.[11] Ferromagnetic impurities were removed via repeated magnetic separation. Although a broad signal centered at 132 ppm remained, it was resolved into two overlapping components at 128 and 144 ppm. These were assigned to semiconducting and metallic nanotubes. In addition, ^{13}C NMR spectroscopy has been exploited in the study of functional groups attached to SWNTs.[13−15]

There have been relatively few theoretical studies of the ^{13}C NMR spectroscopy of nanotubes. Using a tight binding model, Latil et al. studied the London ring current contribution to the shielding tensor of SWNTs.[16] It was concluded that it should be possible to distinguish metallic and semiconducting SWNTs since an 11 ppm shift was predicted. This shift was significant in relation to packing and length dependence effects. Furthermore, a broadening of about 20 ppm was predicted due to the effect of neighboring tubes in a bundle of nanotubes. A later study used density functional theory (DFT) and focused on the (9,0) tube.[17] This work used finite tubes of up to 222 atoms capped with either hydrogen or C_{30}. It was shown that (for finite tubes) the C_{30}-capped tubes provided a better model than the hydrogen-capped ones. A chemical shift of about 130 ppm was predicted.

In this paper, we report quantum mechanical calculations of the ^{13}C NMR spectroscopy of a range of armchair and zigzag nanotubes. A number of issues, such as the sensitivity to length and chirality, are addressed. Finally, the challenges and potential of ^{13}C NMR as a tool for the characterization of nanotubes are discussed.

Computational Details

Following geometry optimization, isotropic ^{13}C nuclear shieldings were computed with the gauge-including atomic orbitals methodology.[18−20] Results are reported as chemical shifts relative to the value for TMS computed at the same level of theory. In this study, we have used Hartree−Fock (HF) theory to determine the shieldings of the carbon atoms. HF theory was chosen primarily to minimize the computational cost of the calculations. HF theory includes no description of electron correlation, and DFT, which does include electron correlation, is usually more accurate. However, DFT provides a poor description of the band gap and a correction is required.[21] To obtain an estimate of the magnitude of the deviation from experiment using HF theory, the chemical shifts for carbon in a test set of "fullerene-like" molecules (shown in Figure 1) were computed using a range of basis sets and compared to experiment. The relatively low computational cost of HF with modest basis sets allows shieldings of all carbons in the tube to be computed and full ^{13}C NMR spectra to be generated. To provide a representation of spectra that may be observed in experiment, the signal arising from each carbon is represented by a Gaussian function. There is no rigorous method to choose the width of these Gaussians. A value for the full width at half-maximum of 8 ppm was chosen through comparison with the available experimental data. This accounts for some of the broadening observed in practical measure-

(13) Chen, J.; Liu, H.; Weimer, W. A.; Halls, M. D.; Waldeck, D. H.; Walker, G. C. *J. Am. Chem. Soc.* **2002**, *124*, 9034−9035.
(14) Kleinhammes, A.; Mao, S.-H.; Yang, X.-J.; Tang, X.-P.; Shimoda, H.; Lu, J. P.; Zhou, O.; Wu, Y. *Phys. Rev. B* **2003**, *68*, 075418.
(15) Ruther, M. G.; Frehill, F.; O'Brian, J. E.; Minett, A. I.; Blau, W. J.; Vos, J. G.; in het Panhuis, M. *J. Phys. Chem. B* **2004**, *108*, 9665−9668.
(16) Latil, S.; Henrard, L.; Goze-Bac, C.; Bernier, P.; Rubio, A. *Phys. Rev. Lett.* **2001**, *86*, 3160−3163.
(17) Zurek, E.; Autschbach, J. *J. Am. Chem. Soc.* **2004**, *126*, 13079−13088.
(18) Ditchfield, R. *Mol. Phys.* **1974**, *27*, 789−807.
(19) Wolinski, K.; Hinton, J. F.; Pulay, P. *J. Chem. Phys.* **1990**, *112*, 8251−8260.
(20) Haser, M.; Ahlrichs, R.; Baron, H. P.; Weiss, P.; Horn, H. *Theor. Chim. Acta* **1992**, *83*, 455−470.
(21) Cioslowski, J.; Rao, N.; Moncrieff, D. *J. Am. Chem. Soc.* **2002**, *124*, 8485−8489.

Table 1. Dimensions of the Nanotubes Studied (HF/STO-3G)

tube	no. of atoms	length (Å)	diameter (Å)
$(4,4)_A$	116	17.40	5.27
$(4,4)_B$	180	27.33	5.30
$(4,4)_C$	212	32.29	5.29
$(4,4)_D$	228	34.70	5.37
$(4,4)_E$	244	37.25	5.27
$(5,5)_A$	140	16.52	6.82
$(5,5)_B$	160	19.06	6.79
$(5,5)_C$	180	21.60	6.77
$(5,5)_D$	220	26.44	6.80
$(5,5)_E$	260	31.40	6.85
$(6,6)_A$	128	13.07	8.28
$(6,6)_B$	164	16.83	8.01
$(6,6)_C$	200	20.53	8.23
$(6,6)_D$	236	24.26	8.19
$(6,6)_E$	272	27.80	8.09
$(6,0)_A$	108	18.08	4.74
$(6,0)_B$	132	22.26	4.92
$(6,0)_C$	156	26.53	4.92
$(6,0)_D$	180	30.79	4.92
$(6,0)_E$	204	35.06	4.79
$(9,0)_A$	150	17.18	7.01
$(9,0)_B$	168	19.32	7.01
$(9,0)_C$	186	21.65	7.03
$(9,0)_D$	222	24.90	7.04
$(9,0)_E$	258	29.17	7.03
$(10,0)_A$	160	16.44	7.83
$(10,0)_B$	180	18.52	7.83
$(10,0)_C$	200	20.65	7.84
$(10,0)_D$	240	24.90	7.87
$(10,0)_E$	280	29.17	7.89

ments. All calculations were performed using the Q-Chem software package.[22]

The (4,4), (5,5), and (6,6) armchair nanotubes and (6,0), (9,0), and (10,0) zigzag nanotubes were studied. For each tube, calculations are reported for a range of different lengths labeled A−E, where E is the longest. The width (at the center of the tube) and length (between the extreme atoms at either end) of these tubes are given in Table 1. The longest tube for each of the different chiralities is shown in Figure 2. The largest of these comprises 280 atoms. There are several ways in which the tubes can be capped. In this study, we have used fullerene fragments; these are shown in Figure 3. The cap for the (9,0) tube has been used in an earlier study.[17] These caps are not unique but have been chosen such that they match the diameter of the tube and also have high symmetry.

Results and Discussion

Table 2 shows the average absolute deviation from experiment (in ppm) for the set of 38 magnetically distinct carbons from the molecules in Figure 1 computed using HF theory in combination with a range of basis sets. These molecules include a range of carbon atoms similar to those found in nanotubes. The results show that the 6-31G, 6-31G*, and cc-pVDZ basis sets all give good agreement with experiment, with an average error of less than 5 ppm. The best results are given by 6-31G*, with an average error of 3.2 ppm. Somewhat surprisingly, HF/STO-3G also gives a low average error of 4.7 ppm. HF/STO-3G also performs relatively well for C_{60} and C_{70}. It should be emphasized that we are reporting chemical shifts with respect to TMS computed at the analogous level of theory. The HF/STO-3G calculations are benefiting from a fortuitous but *consistent* cancellation of errors. However, the low computational cost of HF/STO-3G can be exploited and much larger systems studied. A calculation for a 250 atom nanotube with the STO-3G basis set has a total of 1000 basis functions compared to 3500 basis functions with the 6-31G* basis set. The latter type of calculation is not feasible with our current resources. An HF/STO-3G single-point energy evaluation for the $(5,5)_A$ nanotube takes approximately three-fourths and one-third the time of B3LYP/STO-3G and HF/3-21G calculations, respectively. Consequently, we have chosen to use HF theory with the STO-3G basis set, which should provide a reliable estimate of the chemical shifts.

Table 3 shows the computed band gaps, from which some qualitative observations can be made. Previous DFT calculations on the (5,5) tube[21] observed a slow convergence of the band gap with tube length. The metallic behavior of the infinite tube was approached in an oscillatory manner, and a significant band gap was still present in the longest tubes studied. The HF results for the (5,5) nanotube presented here are consistent with these findings, and a similar behavior is also observed for the smaller and larger diameter armchair nanotubes studied. This strong dependence of the computed band gap on tube length makes it difficult to draw firm conclusions about the limiting values since the computed band gaps are not converged with respect to tube length.

For the (9,0) zigzag tube, earlier DFT work[21] predicted a decrease in band gap with tube length. In addition, it was predicted that the band gap for the (9,0) tube would be finite in the bulk limit. This was in qualitative agreement with experimental studies that show zigzag nanotubes to have finite energy gaps of <0.1 eV.[23] For our calculations, there is generally a significant decrease in the computed band gap as the length of the tube increases. The only exception to this trend is the shortest (6,0) tube. The results presented here indicate that zigzag nanotubes with smaller or larger diameters also show a decreasing band gap with increasing length. Furthermore, the band gap decreases with increasing diameter of the tubes. This feature is also found in experiment, where a dependence of the band gap of zigzag nanotubes with the inverse square of the radius is observed.[23]

Overall, trends in the computed band gaps using HF theory are consistent with those from DFT calculations of the (9,0) and (5,5) tubes.[21] In some respects, HF theory actually outperforms DFT since it is necessary to scale (or shift) the band gap in DFT. This is because DFT tends to underestimate band gaps severely. The corrected DFT (B3LYP/6-311G*) values for a 180 atom (5,5) nanotube and 186 atom (9,0) nanotube are 3.08 and 3.42 eV, respectively. This compares to 3.86 and 5.36 eV predicted by HF/STO-3G. This discrepancy is largely associated with the basis set. Improving the basis set to 3-21G for the smaller nanotubes leads to a decrease in the computed band gaps.

Figures 4 and 5 show simulated ^{13}C NMR spectra for a selection of the zigzag and armchair nanotubes. Initially we will discuss the (9,0) tube. All three spectra for the (9,0) tube show a large peak with a distinct shoulder at higher chemical shift. The locations of the maximum of the larger peaks for all the nanotubes studied are given in Table 4. As the length of the

(22) Kong, J.; et al. *J. Comput. Chem.* **2000**, *21*, 1532−1548.

(23) Ouyang, M.; Huang, J. L.; Cheung, C. L.; Lieber, C. M. *Science* **2001**, *292*, 702.

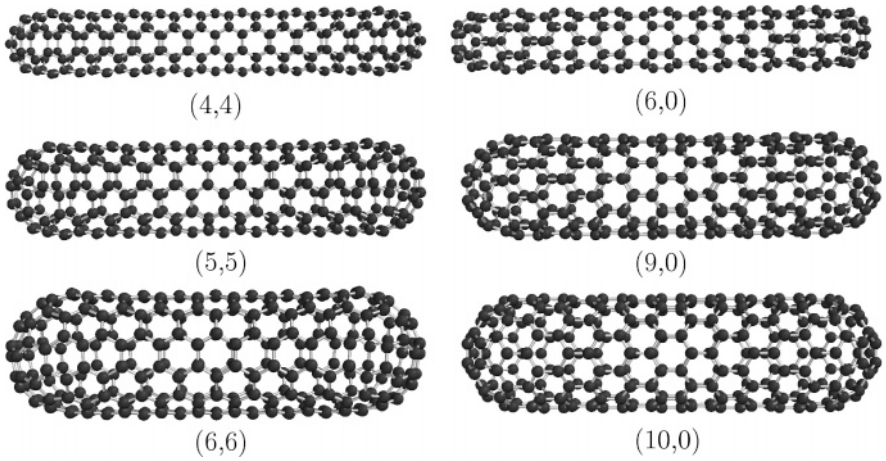

Figure 2. Longest tubes studied.

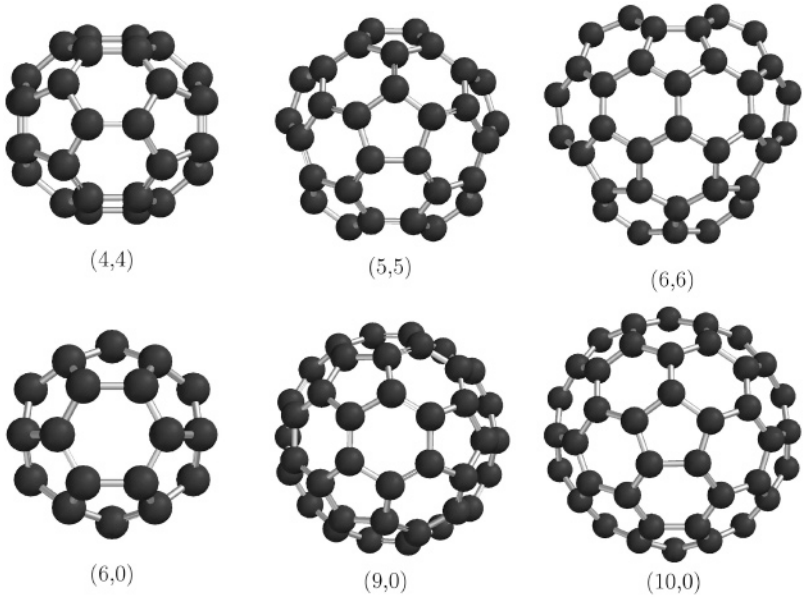

Figure 3. Nanotube caps.

Table 2. Average Absolute Errors in Computed ^{13}C Chemical Shifts in ppm

molecule	STO-3G	3-21G	6-31G	6-31G*	6-311G	6-311G*	cc-pVDZ
benzene	3.7	7.8	3.2	2.2	9.8	10.7	2.5
naphthalene	4.0	8.2	3.1	2.1	9.1	10.7	2.7
azulene	6.6	8.3	3.7	3.9	9.1	9.2	2.1
fluorene	4.2	6.8	3.0	2.1	8.0	9.9	2.6
anthracene	6.0	10.5	2.2	4.5	6.1	7.8	2.1
phenanthracene	3.2	8.0	3.1	1.9	8.8	10.5	2.7
acenaphthylene	4.8	8.4	3.1	3.0	8.1	9.6	8.6
C_{60}	6.5	2.1	11.0	4.3	15.3	16.8	8.5
C_{70}	3.4	5.1	8.5	5.2	13.4	9.4	7.2
ave error	4.7	7.2	4.5	3.2	9.7	10.5	4.3

Table 3. Computed HF/STO-3G Band Gaps in eV[a]

chirality	A	B	C	D	E
(4,4)	5.82 (5.09)	5.44	4.98	4.71	3.76
(5,5)	4.30 (3.95)	5.66	3.86	5.12	4.46
(6,6)	2.23 (2.42)	4.44	1.01	3.95	2.67
(6,0)	4.52 (4.24)	5.42	5.27	5.17	5.06
(9,0)	5.88 (5.20)	4.68	5.36	5.03	4.76
(10,0)	4.27 (3.70)	3.92	4.22	3.76	3.32

[a] HF/3-21G values in parenthesis.

(9,0) tube is increased, there is only a small change in the band position, which moves toward lower chemical shift. For the longest tube, $(9,0)_E$, a chemical shift of 130.1 ppm is predicted. This is in good agreement with the DFT study of Zurek and Autschbach, which found a chemical shift of 133 ppm for the (9,0) tube.[17] This is also consistent with the available experimental data where chemical shifts in the range 116−132 ppm have been reported. As the tube length increases, there is a large change in the relative heights of the two peaks. This is due to the origin of the peaks. Observation of the computed chemical shifts of the carbons show two distinct groups. The carbons comprising the tube have significantly lower chemical shift than those of the caps. Thus the main peak can clearly be assigned to the carbons of the tube, while the smaller peak arises from the carbon atoms in the cap. This smaller peak lies at 149.1 ppm in the $(9,0)_E$ tube which is close to 143 ppm for the carbons in C_{60}. These spectra are similar to those presented by Hayashi et al., where a peak at 152 ppm was observed.[10] This peak was tentatively assigned to carbons at edges or defects. Our calculations indicate that this peak arises from the carbons in the caps. This also raises the possibility that the ratio of the

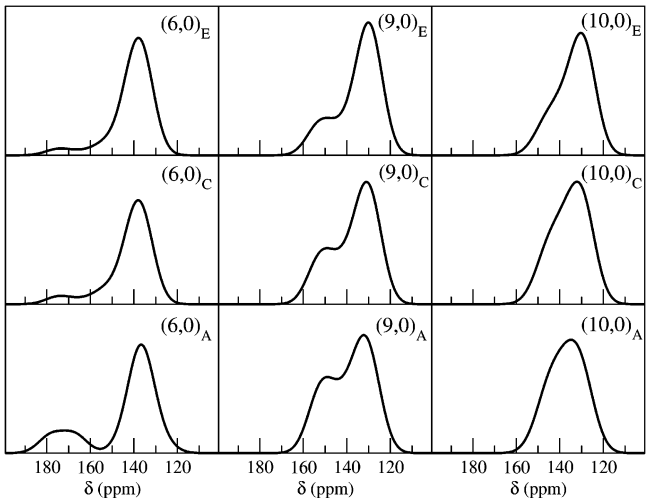

Figure 4. ^{13}C NMR spectra for zigzag nanotubes.

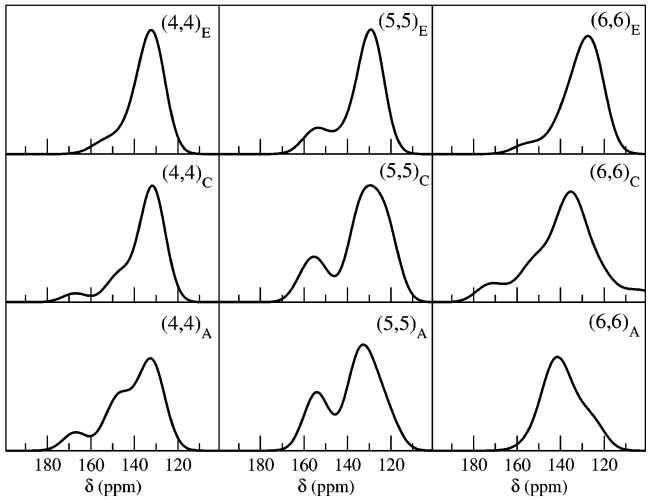

Figure 5. ^{13}C NMR spectra for armchair nanotubes.

Table 4. Position of Maximum Intensity (δ_{max}) in the ^{13}C NMR Spectra in ppm

chirality	A	B	C	D	E
(4,4)	132.7	132.1	131.8	132.9	132.2
(5,5)	132.7	130.2	129.6	129.6	129.3
(6,6)	141.5	134.5	135.3	130.1	127.4
(6,0)	136.6	138.1	138.0	137.9	137.9
(9,0)	132.3	131.1	131.0	130.4	130.1
(10,0)	134.9	133.3	132.1	130.9	130.3

heights of these peaks could be used as a measure of the length of the tube. The comparison of the computed spectra with experiment is complicated by the affects of solvent and aggregation. These factors have been shown to lead to broadening[16] and may also effect the band position. The representation of the spectra in which the signals for each carbon are represented by a Gaussian function provides an approximate account of these broadening effects. However, a detailed study of this is beyond the scope of the present study.

The spectra for the smaller and larger diameter zigzag tubes have a similar structure with a large peak from the carbons in the tube and a smaller peak at larger chemical shift arising from the caps. However, the relative position of the peaks changes giving a band profile characteristic of the type of tube. For (6,0) and (10,0) nanotubes, the cap peaks lie at 175 and 145 ppm, respectively. This difference is a consequence of the nature of the caps. The change in the smaller peak contrasts with that of the larger peak. The position of the main peak for the (6,0) tubes shows little variation with the tube length. For the (10,0) tube, a decrease in the position of maximum intensity as the tube length increases is observed. The greater sensitivity of δ_{max} for the (10,0) tube may arise because the (10,0) tubes studied are further from convergence with respect to length. Comparison of δ_{max} for the different tubes indicates a small decrease as the diameter of the tube increases. A shift of approximately 7 ppm is observed between (6,0) and (10,0) tubes. However, this result should be regarded as qualitative rather than quantitative since the properties of the finite tubes studied may not have converged satisfactorily.

The computed spectra for the (5,5) nanotubes show a pattern similar to that of the (9,0) tubes. The peak due to the tube carbons grows as the length of the tube is increased, and a distinct smaller peak at higher chemical shift arises due to the carbons of the caps. For the $(5,5)_E$ tube the peaks lie at 129.3 and 153.5 ppm. These are close to the corresponding peaks for the (9,0) tube, which lie at 130.1 and 149.1 ppm, respectively. The armchair nanotubes in this study have a finite band gap due to their length. Consequently, the density of states at the Fermi level will be zero resulting in a negligible Knight shift. For armchair nanotubes that have metallic behavior, a Knight shift of approximately 11 ppm is expected.[16] This would result in a total chemical shift of about 140 ppm for the (5,5) tube, which is close to the value expected for metallic tubes. The armchair nanotubes also show a decrease in chemical shift as the diameter of the tubes increases. This shift is approximately 7 ppm between the (4,4) and (6,6) tubes.

Conclusions

Exploitation of the chemical and physical properties of nanotubes requires understanding and control of their structure during synthesis. While several techniques are used to probe nanotube structure, full characterization is not possible. ^{13}C NMR spectroscopy has the potential to provide a more detailed structural characterization. Experimental measurement of ^{13}C NMR spectra of nanotubes is problematic due to residual ferromagnetic impurities from the catalyst used in their synthesis. However, progress to eliminate these impurities has been made and higher resolution obtained.[9,10,12] In this study, we have used ab initio calculations to simulate the ^{13}C NMR spectra of a range of zigzag and armchair nanotubes. It has been shown that a relatively low level of theory (HF/STO-3G) provides relatively accurate chemical shifts for a range of carbons in magnetically similar environments to those that occur in carbon nanotubes. It is reasonable to assume that the same level of theory will provide an adequate description of the ^{13}C NMR of nanotubes while allowing large nanotubes to be studied.

Typically, the computed spectra show two bands. This is consistent with experimental spectra which also show a broad band with a distinct shoulder.[10] The band at lower chemical shift grows with the length of the nanotube and arises from the carbon in the tube. This band shows a weak dependence on the length and width of the nanotube. A shift of about 7 ppm is predicted between the smaller and larger diameter tubes studied here. For tubes of similar diameter and different structure (i.e.,

(5,5) and (9,0)) there is little difference in the position of the band maximum. However, this may change for longer tubes due to differences in the Knight shift. Our calculations indicate that the smaller band at higher chemical shift arises from the carbons in the caps of the nanotube. The location of the band depends on the nature of the cap.

Very high resolution ^{13}C NMR spectra of nanotubes cannot currently be measured. However, these calculations show that the lower resolution band profiles may be rich in structural information. This information is not only in the position of the peak maximum, which may be able to distinguish between different types of nanotube, but also in the shape of the band profile. Information on tube length and diameter may be gleaned from the relative size and position of the smaller peak arising from the caps of the tubes and the larger peak arising from the carbons in the tube.

Acknowledgment. This research was supported by the Engineering and Physical Sciences Research Council through the award of an Advanced Research Fellowship to N.A.B. (GR/R77636). The authors also acknowledge Professor Brian F. G. Johnson for useful discussions.

Supporting Information Available: Complete ref 22. This material is available free of charge via the Internet at http://pubs.acs.org.

JA055888B